Matrix Isolation Study of the Reactions of CrO_2Cl_2 with a Series of Silanes

Nicola Goldberg and Bruce S. Ault*

Department of Chemistry, University of Cincinnati, P.O. Box 210172, Cincinnati, Ohio 45220

Received: September 13, 2005; In Final Form: November 16, 2005

The reactions between CrO_2Cl_2 and a series of silanes have been investigated using matrix isolation infrared spectroscopy. Twin-jet codeposition of the two reagents into argon matrices at 14 K followed by irradiation with light of $\lambda > 300$ nm led to the growth of a number of new bands. These have been assigned to the appropriate silanol species formed by oxygen insertion into the Si−H bond, strongly complexed to $CrCl_2O$. The structures and vibrational frequencies of these complexes have been characterized by high-level theoretical calculations. These calculations also support the relative preference for the insertion reaction compared to other possible pathways. Merged-jet codeposition of SiH_2Cl_2 with CrO_2Cl_2 at 200 °C also led to the formation of the free silanol, $HSiCl_2OH$.

Introduction

The reaction of transition metal compounds with silanes is a known route to the formation of a transition metal−silicon bond.[1,2] Although oxidative addition or metathesis of a Si−H bond in a hydrosilane to a metal center is known for many transition metal elements, the reaction between chromyl chloride, CrO_2Cl_2, and silanes has not been reported. CrO_2Cl_2 is a very strong oxidizing agent, a property that has been utilized extensively for organic synthesis.[3−6] The mechanisms by which these oxidation reactions take place are not well established in many cases. Extensive attempts have been made to theoretically model these reactions.[7−10]

The matrix isolation technique[11−13] was developed to facilitate the isolation and spectroscopic characterization of reactive intermediates and may provide access to the study of initial intermediates in the above reactions. Recent matrix isolation studies from this laboratory have investigated the thermal and photochemical reactions of high-valent transition metal compounds, including $CrCl_2O_2$, with a number of small organic and inorganic substrates.[14−17] Two classes of reactions have been observed to date, the first of which is formation of an initial complex, followed by HCl elimination from the complex and addition of the organic (or inorganic) fragment to the metal center to retain a four-coordinate complex.[14,15] The second is oxygen atom transfer from the metal center to the substrate, leading to an oxidized substrate species.[16−18] This has occurred either through the oxidation of a carbon−carbon multiple bond to a ketone or ketene (e.g., the oxidation of ethyne to ketene[16]) or by expanded valence (e.g., the oxidation[19] of $(CH_3)_2SO$ to $(CH_3)_2SO_2$). When this reaction occurred as a result of irradiation after deposition, the two species (e.g., $CrCl_2O$ and oxidized substrate) then formed a relatively strongly bound complex. The aim of the study was to investigate the reactions of CrO_2Cl_2 with a series of silanes to determine the mechanism(s) of reaction and whether a Cr−Si bond could be formed by this method. High-level theoretical calculations were employed to complement the experimental data.

* Author to whom correspondence should be addressed.

Experimental Section

All the experiments in this study were conducted on a conventional matrix isolation apparatus that has been described previously.[20] Chromyl chloride, CrO_2Cl_2 (Acros Organics), was introduced into the vacuum system as the vapor above the room-temperature liquid, after purification by freeze−pump−thaw cycles at 77 K. $HSiCl_3$, $MeSiCl_3$, $HSiMeCl_2$ (Acros Organics), and $HCCl_3$ (Tedia) were introduced in a similar manner into a separate vacuum manifold and were purified by repeated freeze−pump−thaw cycles at 77 K. SiH_2Cl_2 (Aldrich) was introduced into the vacuum manifold from a lecture bottle and purified by repeated freeze−pump−thaw cycles at 77 K. SiH_4 samples were prepared from a commercial 1% mixture of SiH_4 in argon (Matheson). The mixture was then diluted with additional argon to the desired ratio. Approximately 1 g of the solid $HSiPh_3$ sample (Acros Organics) was placed in a glass sample container which was then placed inside a small oven within the cold cell and gently heated. While the exact temperature of the oven was not known, this method produced a sufficient vapor pressure for $HSiPh_3$ to be deposited onto the cold window. Argon was used as a matrix gas without further purification.

Matrix samples were deposited in both the twin-jet and merged-jet modes. In the former, the two gas samples were deposited from separate nozzles onto the 14 K cold window, allowing for only a brief mixing time prior to matrix deposition. These matrices were then irradiated for 2 or more hours with the H_2O/Pyrex-filtered output of a 200 W medium-pressure Hg arc lamp, after which additional spectra were recorded on a Perkin-Elmer Spectrum One Fourier transform infrared spectrometer at 1 cm^{-1} resolution. In the merged-jet experiments the two deposition lines were joined with an Ultratorr tee at a distance from the cryogenic surface, and the flowing gas samples were permitted to mix and react during passage through the merged region.

Theoretical calculations were carried out using the GAUSSIAN 03 and 03W suites of programs.[21] Density functional calculations using the B3LYP functional were used to locate energy minima, determine structures, and calculate vibrational spectra of potential intermediate species. Final calculations with full geometry optimization employed the 6-311++G(d,2p) basis

10.1021/jp0551723 CCC: $33.50
Published on Web 12/21/2005

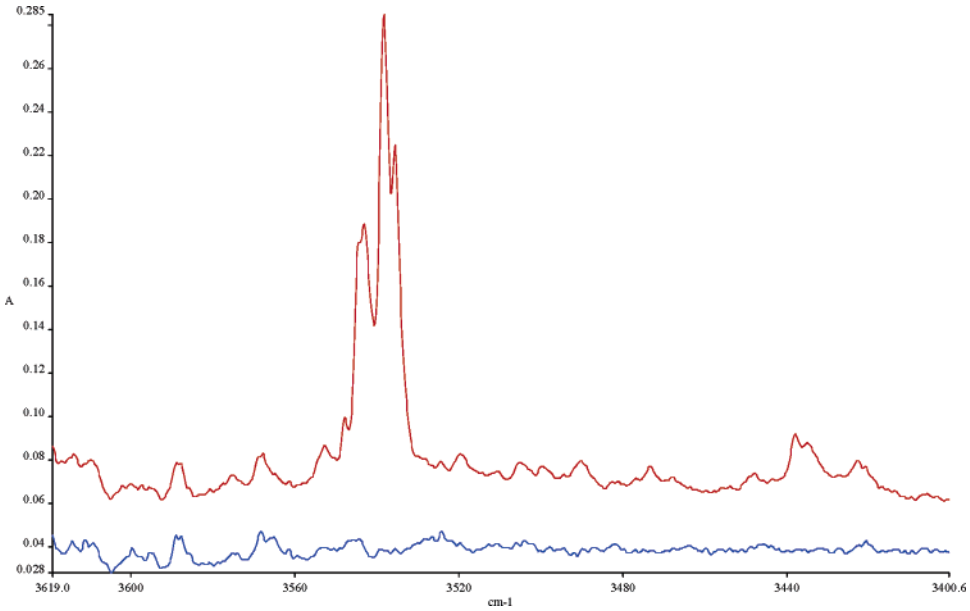

Figure 1. Infrared spectra in the range of 3619−3400 cm^{-1} of matrices prepared by the twin-jet codeposition of a sample of $Ar/CrO_2Cl_2 = 225$ with a sample of $Ar/HSiCl_3$ before (lower trace) and after (upper trace) 4 h of irradiation with light of $\lambda > 300$ nm.

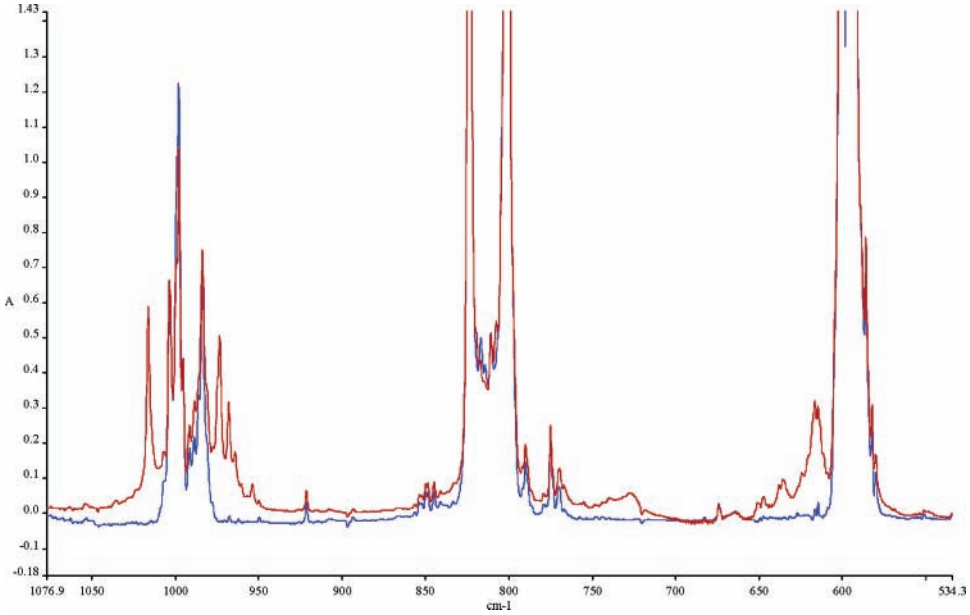

Figure 2. Infrared spectra in the range of 1077−534 cm^{-1} of matrices prepared by the twin-jet codeposition of a sample of $Ar/CrO_2Cl_2 = 225$ with a sample of $Ar/HSiCl_3$ before (lower trace) and after (upper trace) 4 h of irradiation with light of $\lambda > 300$ nm.

set, after initial calculations with smaller basis sets were run to approximately locate energy minima.

Results

Prior to any codeposition experiments, blank experiments were conducted on each of the reagents used in this study. In each case the blanks were in good agreement with literature spectra[22−29] and with blanks run previously in this laboratory. Each blank experiment was then irradiated by the H_2O/Pyrex-filtered output of a 200 W Hg arc lamp for 2 h. No changes were observed in any of these spectra as a result of irradiation.

CrO_2Cl_2 + $HSiCl_3$. In an initial experiment, a sample of $Ar/HSiCl_3 = 225$ was codeposited with a sample of $Ar/CrO_2Cl_2 = 225$ in the twin-jet mode. No distinct new infrared absorptions were apparent upon initial matrix deposition. After irradiation with the H_2O/Pyrex-filtered output of a medium-pressure Hg arc ($\lambda > 300$ nm), new bands were seen at 3538 (center of multiplet), 1016, 973, 727, 640 (center of multiplet), and 436 cm^{-1}. Figure 1 shows the region of the spectrum containing the multiplet near 3538 cm^{-1}, while Figure 2 shows the 1090−515 cm^{-1} region from a representative experiment with this pair of reagents. Table 1 summarizes product band positions for the photochemical products of this reaction.

This experiment was repeated several times, using a range of sample concentrations for each reagent, along with different irradiation times. Similar product bands were seen in all of these experiments, with product band intensities that varied directly with the concentration of the reactants, e.g., when the concentration of one reagent was doubled and the other concentration was held constant, the product band intensities roughly doubled. The product bands also maintained a relatively constant intensity ratio with respect to one another. The optimum conditions were found to be $Ar/HSiCl_3 = 225$ and $Ar/CrO_2Cl_2 = 225$ and 4 h of irradiation.

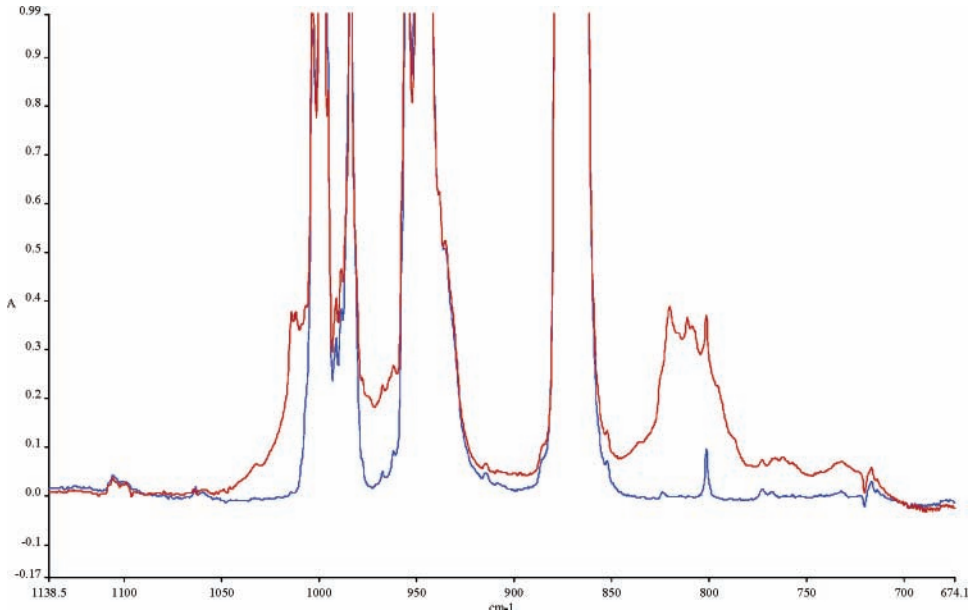

Figure 3. Infrared spectra in the range of 1139−674 cm^{-1} of matrices prepared by the twin-jet codeposition of a sample of $Ar/CrO_2Cl_2 = 125$ with a sample of Ar/SiH_2Cl_2 before (lower trace) and after (upper trace) 4 h of irradiation with light of $\lambda > 300$ nm.

TABLE 1: Calculated and Experimental Band Positions and Assignments for the $CrCl_2O-HOSiCl_3$ Complex[a]

exptl freq	calcd freq[b]	I_{rel}	assignment
3538	3585	0.7	OH str
1016	1139	0.48	CrO str
973	1066	1	OH wag
727	825	0.64	SiO str
640	621	0.63	$SiCl_2$ asym str
436	445	0.17	$SiCl_3$ sym str + $CrCl_2$ asym str

[a] Band positions in cm^{-1}. [b] Calculated bands, unscaled at the B3LYP/6-311++G(d,2p) level.

A series of merged-jet experiments was also undertaken in which the temperature of the merged region ranged from room temperature to 200 °C. No new bands were observed in any of these experiments.

CrO_2Cl_2 + SiH_2Cl_2. When a sample of $Ar/SiH_2Cl_2 = 225$ was codeposited with a sample of $Ar/CrO_2Cl_2 = 125$, and irradiated with light of $\lambda > 300$ nm, a multiplet of new bands was observed between 3400 and 3550 cm^{-1}, the most intense of which was seen at 3547 cm^{-1}. Additional product bands were located at 1031, 1014, 1012, 815 (multiplet), 795 (doublet), 582, and 522 cm^{-1}. Figure 3 shows the 1150−700 cm^{-1} region of the spectrum from a representative experiment with this pair of reagents. This experiment was repeated a number of times, using different sample concentrations. The above results were reproduced in each of these experiments, with product band intensities that varied directly with the concentration of the reactants.

Experiments were also conducted in which the two reagents were deposited in the merged-jet mode. On heating the merged region to 200 °C a series of new bands were seen at 3778, 2889, 942, 864, 813, 811, 748, 607, 582, 571, 568, and 461 cm^{-1}. Table 2 summarizes product band positions for both the photochemical and merged-jet products of CrO_2Cl_2 with SiH_2Cl_2 in argon matrices.

CrO_2Cl_2 + SiH_4. In an initial experiment with this pair of reagents, a sample of $Ar/CrO_2Cl_2 = 150$ was codeposited in the twin-jet mode with a sample of $Ar/SiH_4 = 1000$. No new bands were observed on initial matrix deposition. After irradiating the matrix for 2 h, an intense new band was seen at 3558 cm^{-1}, with weak satellite bands at 3553 and 3520 cm^{-1}.

TABLE 2: Calculated and Experimental Band Positions and Assignments for the $CrCl_2O-HOSiHCl_2$ Complex[a]

merged-jet freq	twin-jet freq	calcd freq[b,c]	calcd freq[b,d]	assignment
3778			3898 (0.53)	OH str
	3547	3671 (0.42)		OH str
2889				HCl str
	1031	1069 (1)		OH wag
	1014,1012	1138 (0.52)		CrO str
942			928 (0.36)	SiO str
864			851 (1)	HSiO bend
	820	815 (0.23)		SiH wag
813,811	815	808 (0.27)	818 (0.63)	SiH wag
	795	804 (0.66)		SiO str
748			756 (0.50)	OH wag
	582	600 (0.56)		$SiCl_2$ asym str
568			563 (0.93)	$SiCl_2$ asym str
	522	525 (0.13)		$SiCl_2$ sym str
461			497 (0.17)	$SiCl_2$ sym str

[a] Band positions in cm^{-1}. [b] Calculated bands, unscaled at the B3LYP/6-311++G(d,2p) level (I_{rel}). [c] For the twin-jet product, the silanol complexed to $CrCl_2O$. [d] For the merged-jet product, the noncomplexed silanol.

Additional product bands were seen at 2223 (multiplet), 1024, 1017, 960, 950 (multiplet), 820, 802, and 459 cm^{-1} as well as a number of weak bands between 700 and 800 cm^{-1}. This initial experiment was repeated several times, with similar results in each experiment. Table 3 summarizes the photochemical product band positions for this reaction.

CrO_2Cl_2 + $HSiMeCl_2$, $HSiPh_3$. On codepositing a sample of $Ar/HSiMeCl_2 = 450$ in the twin-jet mode with a sample of $Ar/CrO_2Cl_2 = 250$ and irradiating them for $4^1/_2$ h, a new multiplet was observed centered at 3547 cm^{-1}. Additional product bands were seen at 1274 (doublet), 1049 (doublet), 1011, 946 (doublet), 938, 824 (doublet), 802(doublet), 738, 592, and 579 cm^{-1}. These results were reproduced in several subsequent experiments. Table 4 summarizes product band positions for the photochemical products of this reaction. A series of merged-jet experiments was also undertaken with these two reagents in which the temperature of the merged region ranged from room temperature to 200 °C. No new bands were observed in any of these experiments.

TABLE 3: Calculated and Experimental Band Positions and Assignments for the $CrCl_2O-HOSiH_3$ Complex[a]

exptl freq	calcd freq[b]	I_{rel}	assignment
3558	3729	0.57	OH str
2225	2305	0.26	SiH_3 asym str
2223	2281	0.30	SiH_2 asym str
2220	2258	0.34	SiH_3 sym str
1024	1094	1	OH rock
1017	1136	0.95	CrO str
952[c]	963	0.72	SiH_2 bend
892[c]	942	0.50	SiH_2 bend
764	765	0.84	SiO str
720	718	0.24	SiH_2 twist
707	695	0.15	SiH_3 wag
459	427	0.79	$CrCl_2$ asym str

[a] Band positions in cm^{-1}. [b] Calculated bands, unscaled at the B3LYP/6-311++G(d,2p) level. [c] Multiplet.

TABLE 4: Calculated and Experimental Band Positions and Assignments for the $CrCl_2O-HOSiMeCl_2$ Complex[a]

exptl freq	calcd freq[b]	I_{rel}	assignment
3547	3677	0.42	OH str
1274	1315	0.08	CH_3 bend
1049	1081	1	OH wag
1011	1134	0.54	CrO str
824	841	0.43	CH_3 rock
802	800	0.25	SiC + SiO asym str
738	732	0.29	SiC + SiO sym str
592, 579	579	0.60	$SiCl_2$ asym str

[a] Band positions in cm^{-1}. [b] Calculated bands, unscaled at the B3LYP/6-311++G(d,2p) level.

TABLE 5: Calculated and Experimental Band Positions and Assignments for the $CrCl_2O-HOSiPh_3$ Complex[a]

exptl freq	calcd freq[b]	I_{rel}	assignment
3567	3679	0.52	OH str
1561	1609	0.01	CH rock
1557	1607	0.01	CH rock
1519	1517	0.01	CH rock
1345	1360	0.01	CH rock
1316	1307	0.03	CCC asym str
1175	1186	0.01	HCCH bend
1162	1185	0.01	HCCH bend
1016	1128	0.64	CrO str
c	1111	1	OH wag
911	875	0.01	CH wag
839	870	0.01	CH wag
789	760	0.02	CH wag
571	632	0.01	CCC bend
527	540	0.55	OH wag
513	503	0.08	OH rock
437	415	0.23	$CrCl_2$ asym str

[a] Band positions in cm^{-1}. [b] Calculated bands, unscaled at the B3LYP/6-311++G(d,2p) level. [c] Peak obscured by a strong parent band.

In an initial twin-jet experiment, $Ar/HSiPh_3$ was codeposited with a sample of $Ar/CrO_2Cl_2 = 250$. No distinct new infrared absorptions were apparent upon initial matrix deposition. On irradiation for 16 h new bands were seen at 3567, 1561 (doublet), 1519(br), 1345, 1316, 1175, 1162, 1016(sh), 911, 839-(sh), 789(sh), 571(br), 527, 513(sh), and 437 cm^{-1}. These results were also reproduced in several additional experiments. Table 5 summarizes the photochemical product band positions for this reaction.

CrO_2Cl_2 + $HCCl_3$, $MeSiCl_3$. A twin-jet experiment was undertaken in which a sample of $Ar/HCCl_3 = 225$ was codeposited with a sample of $Ar/CrO_2Cl_2 = 150$ and irradiated for 4 h. No distinct new infrared absorptions were apparent either upon initial matrix deposition or on irradiation. $Ar/CrO_2Cl_2 = 225$ was also codeposited with $Ar/MeSiCl_3 = 450$ in the twin-jet mode and irradiated for 4 h. No new bands were observed upon initial matrix deposition or on irradiation.

Additional experimental spectra for all of these systems are presented in Figures S1−S8 of the Supporting Information.

Results of Calculations

On the basis of previous studies, a number of different products might be formed either thermally or photochemically. These include oxygen atom addition and insertion reactions, as well as HCl elimination from an initial complex to form a Si−Cr bonded species. As will be discussed below, the most likely pathway for these reactions involves oxygen insertion into the silicon−hydrogen bond where the resulting silanol complexes to the $CrCl_2O$ species (except in the $CrCl_2O_2/Cl_2SiH_2$ merged-jet experiments, where uncomplexed $Cl_2Cr(H)OH$ would be formed). DFT calculations were undertaken on all of these silanol species using the B3LYP hybrid functional and basis sets as high as 6-311++G(d,2p). In addition, weakly bonded intermediate 1:1 complexes between the two reactants were calculated. All of these species optimized to energy minima on the potential energy surface, with all-positive vibrational frequencies. Figure 4 shows the relative energies and calculated structures for the reaction of CrO_2Cl_2 with $HSiCl_3$, while Figure 5 shows the equivalent diagram for the $CrO_2Cl_2-SiH_2Cl_2$ system. Finally, these same properties were calculated for the HCl elimination product for the $CrCl_2O_2-HSiCl_3$ system, $ClCr(O)_2SiCl_3$, and the oxygen addition product $Cl_3HSiO-CrCl_2O$. Additional computational results are presented in Figures S9−S13 of the Supporting Information.

Discussion

Twin-jet codeposition of CrO_2Cl_2 with $HSiCl_3$, SiH_2Cl_2, $HSiMeCl_2$, $HSiPh_3$, and SiH_4 into argon matrices did not lead initially to any distinct new product bands, a result that is typical of twin-jet reactions. After irradiation of these matrices with light of $\lambda > 300$ nm, new product bands were detected in each case. For a photochemical reaction to occur under these experimental conditions, the two reagents must be trapped within the same cage or site, either through a statistical distribution of species during the deposition process or through the formation of weakly bound complexes that were not themselves detected spectroscopically. For a given pair of reagents, using several different sample concentrations, only a single set of product bands was detected. This indicates that only a single product is formed, independent of the initial sample concentrations (over the range sampled in these experiments). In as much as these were relatively dilute experiments (Ar/reagent as high as 500/1), it is very likely that the stoichiometry of the cage pair/weak complex is 1:1, i.e., one molecule of CrO_2Cl_2 and one molecule of the respective silane. Moreover, as will be described below, the product bands fit very well to the calculated spectrum for one of the likely products from a 1:1 reaction.

Two mechanisms for similar photoreactions have been seen to date, one involving HCl elimination, with addition of the substrate species to the chromium center, and the other involving oxygen transfer from $CrCl_2O_2$ to the substrate. No evidence was observed in the region of 2700−2900 cm^{-1} for the formation of HCl, which would have been the eliminated molecule if a Cr−Si bonded product were to form. DFT calculations support this conclusion in that the calculated energy, relative to that of the reactants, of the HCl eliminated product for the $HSiCl_3$ reaction is endothermic at +12.5 kcal mol^{-1} (see Figure 4). In

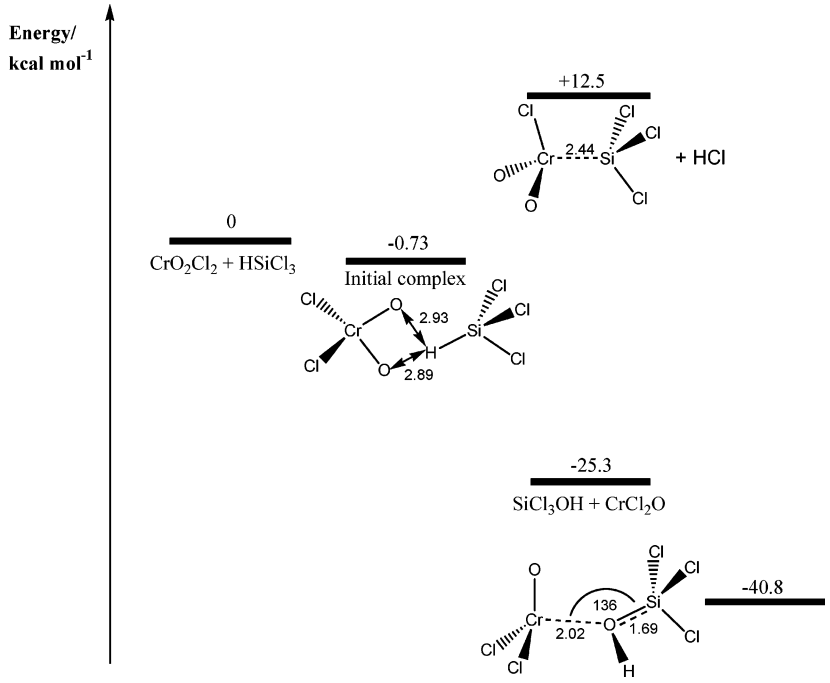

Figure 4. DFT B3LYP/6-311++G(d,2p) calculated structures of the reaction products of CrO_2Cl_2 with $HSiCl_3$. Selected distances are given in angstroms and angles in deg.

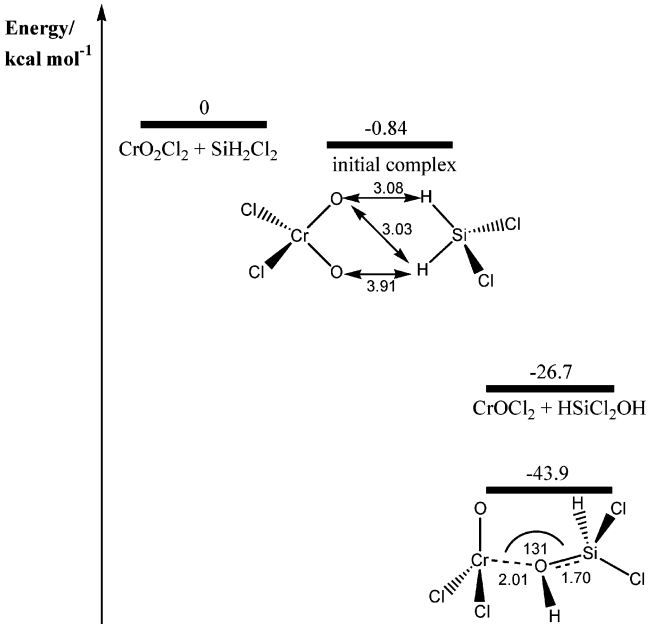

Figure 5. DFT B3LYP/6-311++G(d,2p) calculated structures of the reaction products of CrO_2Cl_2 with SiH_2Cl_2. Selected distances are given in angstoms and angles in deg.

addition, the observed product bands were not consistent with the HCl elimination product $Cl_3Si-CrClO_2$. Consequently, the HCl elimination pathway can be ruled out.

Evidence for oxygen atom transfer would come from both the formation of an oxidized substrate and formation of the $CrCl_2O$ species. In each experiment, product bands (or in the more concentrated experiments, shoulders) were observed near 1016 and 460 cm^{-1}. These are close to, but do not match, the spectral features of parent $CrCl_2O_2$. However, these bands match very well the known band positions of the $CrCl_2O$ species.[30,31] Since these bands were consistent across all of the experiments in this study, and agree with the literature spectrum of $CrCl_2O$, they are so assigned. This clearly indicates that oxygen transfer to the substrate has taken place.

The identity of the oxidized substrate may be deduced from the remaining product bands. In particular, a strong new band was seen in each experiment near 3550 cm^{-1}, which is strongly indicative of an OH stretching mode. This demonstrates that for each parent silane, the oxygen atom has inserted into the Si−H bond to form a silanol. The two products of the irradiation, $CrCl_2O$ and the silanol, are then trapped within the same matrix cage. In as much as the chromium center is quite electron deficient, it is very likely that the two species will interact and form a molecular complex. This result is also supported by DFT calculations. Calculations indicate that the molecular complex is more stable than the separated products, for example by approximately 15 kcal mol^{-1} for the $Cl_3SiOH/CrCl_2O$ complex, and are stabilized by an interaction between one of the lone pairs on the silanol oxygen and the chromium center. The structures of these complexes are shown for the $HSiCl_3$ and SiH_2Cl_2 reactions in Figures 4 and 5.

The calculated vibrational frequencies for these complexes are listed in Tables 1−5 and compared there to the experimental frequencies. Overall, the agreement is quite good. For example, the O−H stretching mode for the $Cl_3SiOH/CrCl_2O$ complex is calculated at 3585 cm^{-1}, unscaled, at the B3LYP/6-311++g-(d,2p) level of theory, which is in good agreement with the experimental value of 3536 cm^{-1}, when anharmonicity is taken into account. A similar level of agreement was found for each of the product bands for each of the silanol/$CrCl_2O$ complexes that were formed, which strongly supports assignment to each silanol product. This result, the insertion of an O atom from $CrCl_2O_2$ into an Si−H bond, represents the first example an insertion reaction from $CrCl_2O_2$ and suggests the possibility of photochemical bond activation by $CrCl_2O_2$. Previous examples had all involved addition reactions, such as the oxidation of C_2H_2 to H_2CCO, complexed to $CrCl_2O$.

Three of the product silanols have been observed by other researchers, although not complexed to $CrCl_2O$, while two of the silanols are new species. The effect of complexation is quite apparent, both in the calculations and in comparison of the complexed silanol to the three known silanols. For example,

Shirk and Shirk[32] reported the O−H stretching mode of $SiCl_3OH$ in solid argon at 3693 cm^{-1}, compared to the 3536 cm^{-1} position observed here. This shift of 157 cm^{-1} can be attributed to complexation with $CrCl_2O$ and is actually somewhat smaller than the calculated shift of 310 cm^{-1} from the free to complexed Cl_3SiOH. Similarly, the solution phase value for the OH stretch of Ph_3SiOH is reported to be 3678[33,34] compared with the band observed here which has shifted to 3567 cm^{-1}. For SiH_3OH, Withnall and Andrews[35] have observed the OH stretch of this species at 3661 cm^{-1} compared with the band observed in these experiments at 3558 cm^{-1}. These shifts, somewhat greater than 100 cm^{-1}, are reasonable and expected upon formation of a relatively strong complex between the Cr and the oxygen atom of the silanol.

The calculations also predict the formation of stable 1:1 complexes between $CrCl_2O_2$ and each of the parent silanes. These are calculated to be very weakly bound, on the order of 1 kcal mol^{-1} binding energy with respect to the separated reagents, as shown in Figures 4 and 5 and the Supporting Information. In addition, the vibrational frequencies calculated for the complex all lie very close to vibrational modes of the isolated parent species, which is consistent with the lack of observation of the complexes experimentally (i.e., that the weak complex bands are hidden by the intense, overlapping parent bands). Nonetheless, it is not surprising that the complexes should be stable, and it is the photochemistry of these complexes that leads to silanol formation.

The merged-jet reaction of CrO_2Cl_2 with SiH_2Cl_2 at 200 °C leads to the observation of several new bands. A product band can be seen in the OH stretching region at 3778 cm^{-1} as well as other new bands in the lower part of the spectrum. No CrO_2Cl_2 peaks are visible, indicating reaction and/or decomposition on the wall of the deposition line at this elevated temperature. The bands in the O−H stretching region, although weak, suggest the formation of $HSiCl_2OH$ not complexed to $CrCl_2O$. The position of these bands, and those in the lower region of the spectrum, are consistent with frequencies calculated for free $HSiCl_2OH$. A new band was also seen at 2889 cm^{-1} which can reasonably be assigned to isolated HCl. This is likely formed through the reaction of CrO_2Cl_2 with impurity water vapor in the merged region, as has been seen previously, than from a product of the silane reaction. The product peaks seen in the merged-jet experiments therefore can be assigned to the free silanol, $HSiCl_2OH$, rather than the silanol complexed to $CrCl_2O$ observed in the twin-jet reaction.

On the basis of previous photochemical reactions of $CrCl_2O_2$ with organic and inorganic substrates, $Cl_3SiCrClO_2$ and Cl_3HSiO might have been expected to form in the reaction with $HSiCl_3$. They were not observed, while the silanol insertion product was seen. The calculated energetics shown in Figure 4 support this finding, as the reaction to form Cl_3SiOH and $CrCl_2O$ is predicted to be the most energetically favorable of the possible reactions. This is likely due to the relatively high affinity of silicon for oxygen, the relatively low bond strength of the Si−H bond, and the polarity of the Si−H bond.

To explore these issues further, two additional systems were studied. First, the reaction between CrO_2Cl_2 and $HCCl_3$ was examined in order to see whether oxygen insertion would occur with a C−H bond as it did with the Si−H bond. No product bands were detected in these experiments after irradiation, indicating that insertion in a C−H bond does not occur under these conditions. In addition, calculations for the reaction of $CrCl_2O_2 + HCCl_3 \rightarrow CrCl_2O{-}HOCCl_3$ complex predict the product to be stable by just 1.74 kcal mol^{-1} relative to the reactants. This compares with the calculated energies for the silane complexes of around −40 kcal mol^{-1}. The weakness of the Si−H bond compared to the C−H bond and the polarity of the Si−H bond must make oxygen insertion more favorable than the essentially nonpolar C−H bond.

The second reaction was that of $CrCl_2O_2$ with H_3CSiCl_3 to explore the possible insertion of an O atom into a Si−C bond. For this system also, no product bands were observed before or after irradiation. Calculations predict this reaction, to form the $H_3COSiCl_3{-}CrCl_2O$ complex, to be relatively favorable, with the product complex 11.7 kcal mol^{-1} below the reactants. Nonetheless, reaction did not occur. It is likely that steric factors play a role here as the bulky methyl group would make it much more difficult for the oxygen atom to insert into the Si−C bond. Also, the Si−C bond is less polar than the Si−H bond in the silanes.

Conclusions

The photochemical reactions of CrO_2Cl_2 with $HSiCl_3$, SiH_2Cl_2, $HSiMeCl_2$, $HSiPh_3$, and SiH_4 in argon matrices following twin-jet deposition led to oxygen insertion to form a series of silanol−$CrCl_2O$ complexes. High-level density functional calculations supported the formation and stability of these species, and the computed vibrational frequencies were in good agreement with the experimental frequencies, when anharmonicity was taken into account. *This is the first observation of an insertion reaction with CrO_2Cl_2.* The insertion reaction was calculated to be more energetically favorable than either the oxygen addition reaction or the HCl elimination reaction. The merged-jet deposition of CrO_2Cl_2 with SiH_2Cl_2 at 200 °C led to the observation of the free silanol, $HSiCl_2OH$.

Acknowledgment. The National Science Foundation is gratefully acknowledged for support of this research through Grant CHE 02-43731. The Ohio Supercomputer center is also acknowledged for computational time.

Supporting Information Available: Additional spectra as well as additional calculated structures and energies for all of the systems presented here. This material is available free of charge via the Internet at http://pubs.acs.org.

References and Notes

(1) Corey, J. Y.; Braddock-Wilking, J. *Chem. Rev.* **1999**, *99*, 175.
(2) Lin, Z. *Chem. Soc. Rev.* **2002**, *31*, 239.
(3) Sharpless, K. B.; Teranishi, A. Y.; Bäckvall, J.-E. *J. Am. Chem. Soc.* **1977**, *99*, 3120.
(4) Cook, G. K.; Mayer, J. M. *J. Am. Chem. Soc.* **1994**, *117*, 7139.
(5) Limberg, C. *Chem. Eur. J.* **2000**, *6*, 2083.
(6) Rappe, A. K.; Jaworska, M. *J. Am. Chem. Soc.* **2003**, *125*, 13956.
(7) Torrent, M.; Deng, L.; Duran, M.; Sola, M.; Ziegler, T. *Can. J. Chem.* **1999**, *77*, 1476.
(8) Torrent, M.; Deng, L.; Ziegler, T. *Inorg. Chem.* **1998**, *37*, 1307.
(9) Ziegler, T.; Li, J. *Organometallics* **1995**, *14*, 214.
(10) Deng, L.; Ziegler, T. *Organometallics* **1997**, *16*, 716.
(11) Cradock, S.; Hinchcliffe, A. J. *Matrix Isolation*; Cambridge University Press: Cambridge, 1975.
(12) Hallam, H. E. *Vibrational Spectroscopy of Trapped Species*; John Wiley & Sons: New York, 1973.
(13) Andrews, L., Moskovits, M., Eds. *Chemistry and Physics of Matrix-Isolated Species*; Elsevier Science Publishers: Amsterdam, 1989.
(14) Ault, B. S. *J. Am. Chem. Soc.* **1998**, *120*, 6105.
(15) Subel, B. L.; Kayser, D. A.; Ault, B. S. *J. Phys. Chem. A* **2002**, *106*, 4998.
(16) Ault, B. S. *J. Phys. Chem. A* **2004**, *108*, 5537.
(17) Goldberg, N.; Lubell, S. R.; Ault, B. S. *J. Mol. Struct.* **2005**, *740*, 125.
(18) Kayser, D. A.; Ault, B. S. *J. Phys. Chem. A* **2003**, *107*, 6500.
(19) Griner, G. M.; Kayser, D. A.; Ault, B. S. *Chem. Phys.* **2004**, *300*, 63.

(20) Ault, B. S. *J. Am. Chem. Soc.* **1978**, *100*, 2426.
(21) Frisch, M. J.; Trucks, G. W.; Schlegel, H. B.; Robb, M. A.; Cheeseman, J. R.; Montgomery, J., J. A.; Vreven, T.; Kudin, K. N.; Burant, J. C.; Millam, J. M.; Iyengar, S. S.; Tomasi, J.; Barone, V.; Mennucci, B.; Cossi, M.; Scalmani, G.; Rega, N.; Petersson, G. A.; Nakatsuji, H.; Hada, M.; Ehara, M.; Toyota, K.; Fukuda, R.; Hasegawa, J.; Ishida, M.; Nakajima, T.; Honda, Y.; Kitao, O.; Nakai, H.; Klene, M.; Li, X.; Knoz, J. E.; Hratchian, H. P.; Cross, J. B.; Adamo, C.; Jaramillo, J.; Gomperts, R.; Stratmann, R. E.; Yazyev, O.; Austin, A. J.; Cammi, R.; Pomelli, C.; Ochterski, J. W.; Ayala, P. Y.; Morokuma, K.; Voth, G. A.; Salvador, P.; Dannenberg, J. J.; Zakrzewski, V. G.; Dapprich, S.; Daniels, A. D.; Strain, M. C.; Farkas, O.; Malick, D. K.; Rabuck, A. D.; Raghavachari, K.; Foresman, J. B.; Ortiz, J. V.; Cui, Q.; Baboul, A. G.; Clifford, S.; Cioslowski, J.; Stefanov, B. B.; Liu, G.; Liashenko, A.; Piskorz, P.; Komaromi, I.; Martin, R. L.; Fox, D. J.; Keith, T.; Al-Laham, M. A.; Peng, C. Y.; Nanayakkara, A.; Challacombe, M.; Gill, P. M. W.; Johnson, B.; Chen, W.; Wong, M. W.; Gonzalez, C. and Pople, J. A. *Gaussian 03*, revision B.04; Gaussian Inc.: Pittsburgh, PA, 2003.
(22) Varetti, E. L.; Müller, A. *Spectrochim. Acta, Part A* **1978**, *34*, 895.
(23) Jeng, M.-L. H.; Ault, B. S. *Inorg. Chem.* **1990**, *29*, 837.
(24) Milligan, D. E.; Jacox, M. E. *J. Chem. Phys.* **1968**, *49*, 1938.
(25) King, S. T. *J. Chem. Phys.* **1968**, *49*, 1321.
(26) Brown, J. D.; Tevault, D.; Nakamoto, K. *J. Mol. Struct.* **1977**, *40*, 43.
(27) Durig, J. R.; Hawley, C. W. *J. Chem. Phys.* **1973**, *58*, 237.
(28) Kaplan, L. *J. Am. Chem. Soc.* **1954**, *76*, 5880.
(29) Wilde, R. E.; Srinivasan, T. K. K.; Harral, R. W.; Sankar, S. G. *J. Chem. Phys.* **1971**, *55*, 5681.
(30) Ault, B. S. *J. Phys. Chem. A* **2004**, *108*, 5537.
(31) Wistuba, T.; Limberg, C. *Eur. J. Inorg. Chem.* **1999**, 1355.
(32) Shirk, A. E.; Shirk, J. S. *J. Mol. Spectrosc.* **1982**, *92*, 218.
(33) Matwiyoff, N. A.; Drago, R. S. *J. Organomet. Chem.* **1965**, *3*, 393.
(34) West, R.; Baney, R. H.; Powell, D. L. *J. Am. Chem. Soc.* **1960**, *82*, 6269.
(35) Withnall, R.; Andrews, L. *J. Phys. Chem.* **1985**, *89*, 3261.